Lucena et al., http://www.jcb.org/cgi/content/full/jcb.201412144/DC1

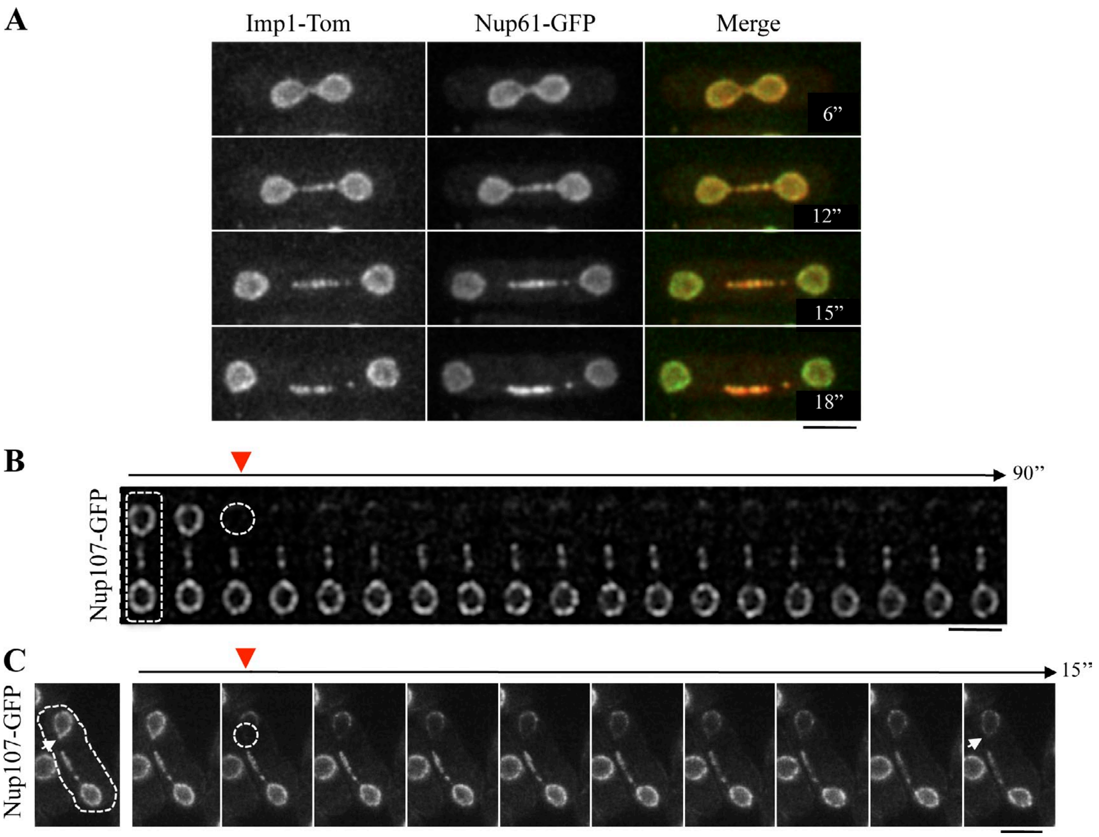

Figure S1. **Imp1-Tom and Nup61-GFP colocalization and Nup107-GFP dynamics in the nuclear envelope of anaphase B cells.** (A) Colocalization of Imp1-Tom and the nuclear pore marker Nup61-GFP by time-lapse fluorescence microscopy. (B) Time-lapse images of a representative Nup107-GFP–expressing cell (dashed line). Red arrowhead indicates image acquired immediately after photobleaching one entire nucleus. (C) As in B but photobleaching the half nuclear region flanking the internuclear bridge. White arrows indicate a possible barrier that restricts free diffusion of nuclear pores from the nuclear membrane to the bridge membrane before and after photobleaching. Bars, 5 µm.

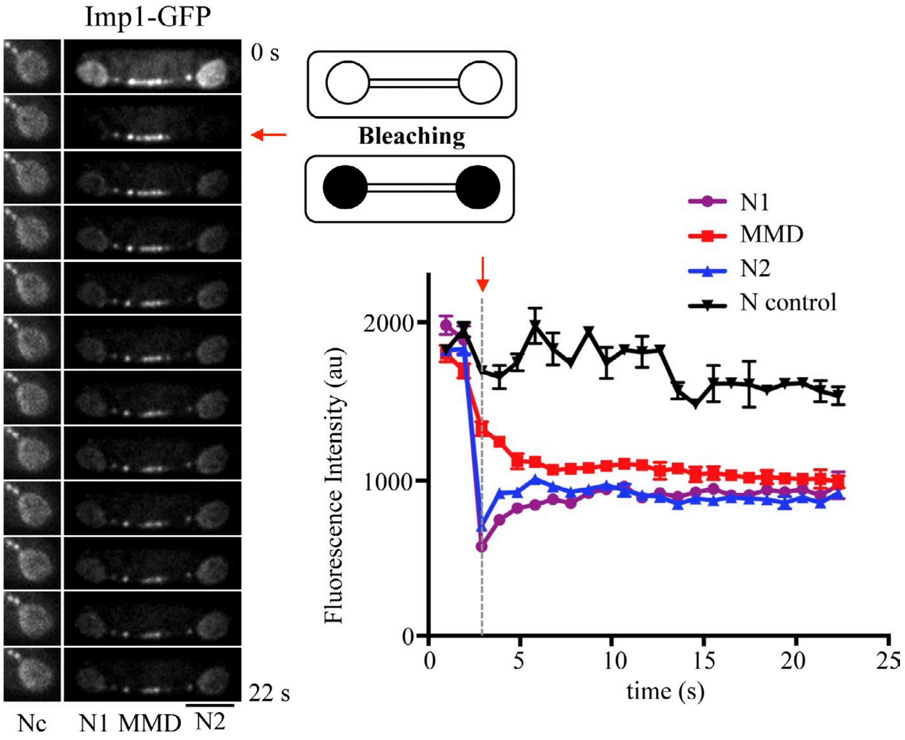

Figure S2. **Time-lapse fluorescence images of Imp1-GFP–expressing cells.** Red arrow indicates image acquired immediately after photobleaching Imp1-GFP in the two nuclei (see schematized cells on right). (graph) Time course fluorescence intensity (FLIP assay, arbitrary units) in both nuclei and the MMD region (N1, N2 and MMD, respectively). Time immediately after photobleaching is indicated by the red arrow and dashed line. Nonbleached nucleus is used as a control. Bar, 5 µm

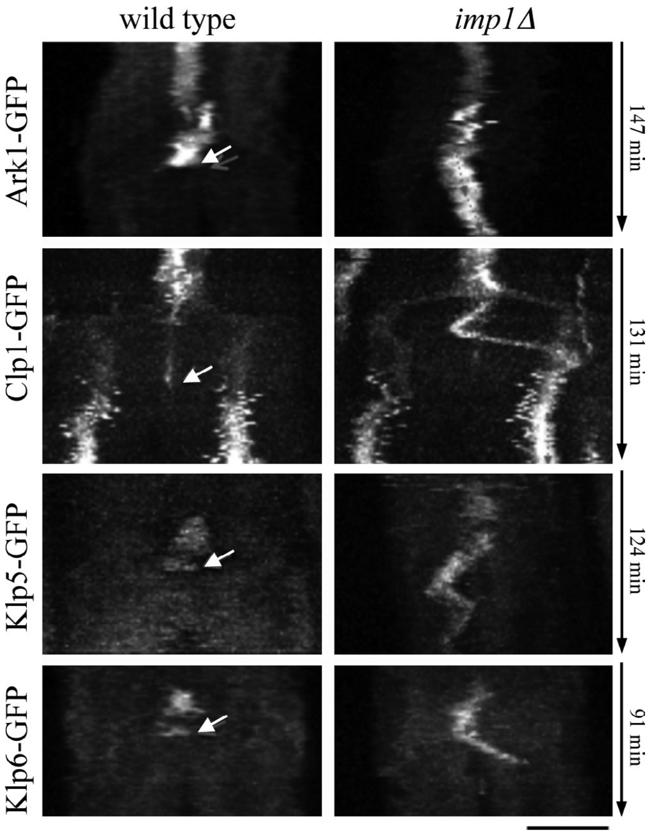

Figure S3. **Kymographs of wild-type and *imp1Δ* cells expressing Ark1-GFP (Aurora B) kinase, Clp1-GFP phosphatase, and Klp5-GFP and Klp6-GFP kinesins.** Arrows indicate spindle disassembly in wild-type cells. Bar, 5 µm

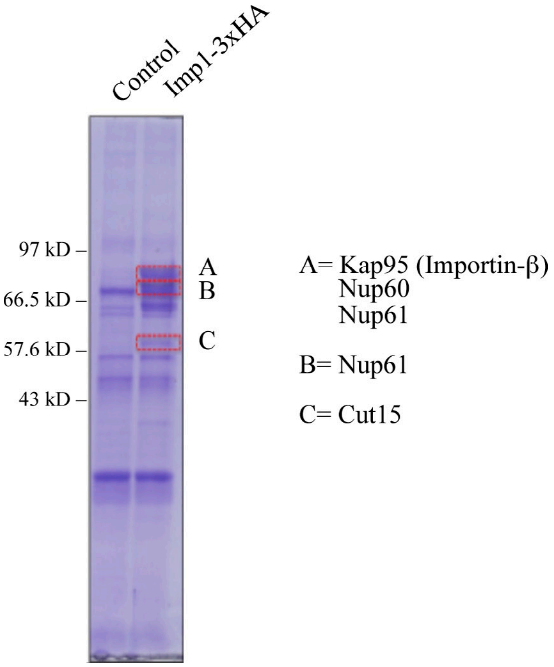

Figure S4. **Imp1–3xHA–associated proteins (Coomansie blue staining) separated by SDS-PAGE.** A, B, and C represent abundant Imp1–3xHA–binding proteins a compared with the control.

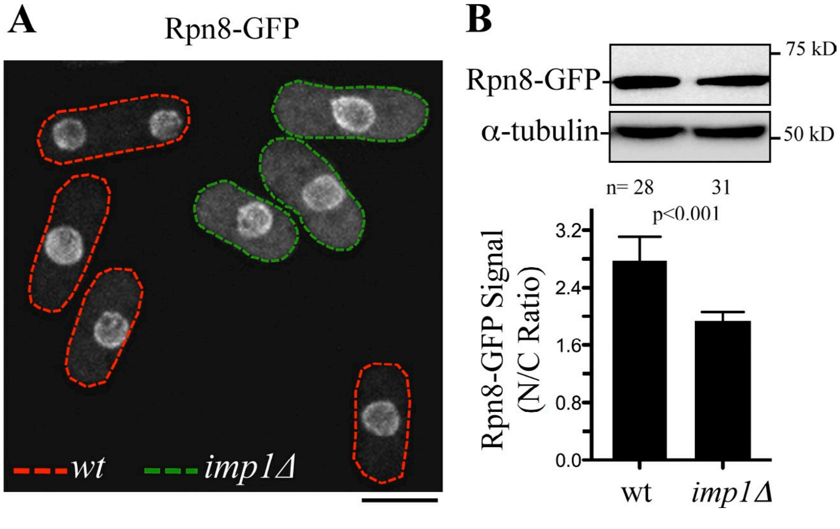

Figure S5. **Influence of Imp1 in the nuclear localization of the Rpn8 proteasome regulatory factor.** (A) Rpn8-GFP localization in asynchronous *rpn8-GFP* (lectin labeled) and *rpn8-GFP imp1Δ* cells (green- and red-dashed cells, respectively) incubated at 25°C. Bar, 5 µm. (B) Ratio of nuclear to cytoplasmic fluorescence intensity in asynchronous *rpn8-GFP* (lectin labeled) and *rpn8-GFP imp1Δ* cells. Western blot analysis of Rpn8-GFP in cell extract of both strains are shown. Tubulin is used as a control. Graph represents mean and standard deviation.

Table S1. **Imp1–3xHA binding proteins identified by mass spectrometry**

PomBase accession no.	Gene	Imp1–3xHA	Control	Protein description
SPCC18B5.07c	**nup61**	**53**	**6**	**Nucleoporin**
SPCC285.13c	**nup60**	**43**	**2**	**Nucleoporin**
SPAC30D11.04c	**nup124**	**27**	**0**	**Nucleoporin**
SPBC19C7.10	bqt4	11	0	Bouquet formation protein
SPAC1B1.03c	kap95	10	0	Karyopherin
SPBC1604.08c	**imp1**	**9**	**1**	**Importin-α**
SPCC895.05	for3	9	1	Formin
SPCC13B11.01	adh1	8	3	Alcohol dehydrogenase
SPAC13G7.02c	ssa1	7	3	Heat shock protein Ssa1 (predicted)
SPBC1773.09c	mug184	5	0	Hsp70 protein binding protein
SPAC1071.08	rpp203	5	2	60S acidic ribosomal protein P2C subunit
SPCC1840.02c	bgs4	5	2	1,3-β-glucan synthase subunit Bgs4
SPBC9B6.08	clc1	5	3	Clathrin light chain
SPBC106.06	cct4	4	0	Chaperonin-containing T-complex δ subunit Cct4
SPCC965.05c	thp1	4	0	Uracil DNA *N*-glycosylase
SPCC962.03c	**cut15**	**4**	**0**	**Karyopherin**
SPAC26F1.03	pda1	4	0	Pyruvate dehydrogenase e1 component α subunit
SPAC1F5.02	pdi1	4	0	Protein disulfide isomerase (predicted)
SPCC1795.11	sum3	4	1	Translation initiation RNA helicase
SPAC11E3.15	rpl22	4	1	60S ribosomal protein L22 (predicted)
SPAC2F3.06c	**kap104**	**3**	**0**	**Karyopherin**
SPBC17D11.05	tif32	3	0	Translation initiation factor eIF3a
SPCC417.08	tef3	3	0	Translation elongation factor eEF3
SPBC2G2.08	ade9	3	0	C-1-tetrahydrofolatesynthase (predicted)
SPBC365.03c	rpl2101	3	1	60S ribosomal protein L21 (predicted)
SPBC56F2.02	rpl1901	3	1	60S ribosomal protein L19
SPCC825.01	Unassigned	3	1	Ribosome biogenesis ATPase, Arb family ABCF1-like
SPBC776.15c	kgd2	3	1	Dihydrolipoamide *S*-succinyltransferase (predicted)
SPBC646.10c	Unassigned	3	1	U3 snoRNP protein Nop56 (predicted)
SPBC405.05	atg16	3	1	Autophagy protein
SPCC794.07	lat1	3	1	Dihydrolipoamide *S*-acetyltransferase E2 (predicted)
SPBP8B7.06	rpp201	2	1	60S acidic ribosomal protein A2
SPBC30D10.13c	pdb1	2	0	Pyruvate dehydrogenase e1 component β subunit
SPCP1E11.09c	rpp103	2	0	60S acidic ribosomal protein
SPAC890.08	rpl31	2	0	60S ribosomal protein L31 (predicted)
SPAC3H5.12c	rpl501	2	0	60S ribosomal protein L5 (predicted)
SPAC589.06c	Unassigned	2	0	pho88 family protein (predicted)
SPBC3B9.13c	rpp102	2	0	60S acidic ribosomal protein
SPBC16A3.08c	oga1	2	0	Stm1 homolog
SPBC29A3.16	rrs1	2	0	Ribosome biogenesis protein (predicted)
SPBC215.06c	Unassigned	2	0	human LYHRT homolog
SPAC17H9.04c	Unassigned	2	0	RNA-binding protein
SPBC2G5.06c	hmt2	2	0	Sulfide-quinone oxidoreductase
SPBC4C3.05c	nuc1	2	0	DNA-directed RNA polymerase I complex large subunit
SPAC22G7.05	kri1	2	0	Ribosome biogenesis protein Kri1 (predicted)
SPBP4H10.15	Unassigned	2	0	Aconitate hydratase
SPBC13A2.04c	ptr2	2	0	PTR family peptide transmembrane transporter
SPCC1682.16	**rpt4**	**2**	**1**	**19S proteasome regulatory subunit (predicted)**
SPCC364.06	nap1	2	1	Nucleosome assembly protein Nap1
SPBC839.04	rpl803	2	1	60S ribosomal protein L8 (predicted)
SPCC1183.08c	rpl101	2	1	60S ribosomal protein L10a
SPAC1420.03	**rpn501**	**2**	**1**	**19S proteasome regulatory subunit**
SPCC1682.10	**rpn8**	**1**	**0**	**19S proteasome regulatory subunit (predicted)**
SPAC589.10c	Unassigned	1	0	Ribosomal-ubiquitin fusion protein Ubi5 (predicted)
SPBC3E7.02c	hsp16	1	0	Heat shock protein
SPAC1565.08	**cdc48**	**1**	**0**	**AAA family ATPase involved in protein degradation**
SPBC26H8.08c	grn1	1	0	GTPase Grn1
SPBC582.07c	**rpn7**	**1**	**0**	**19S proteasome regulatory subunit**

Table S1. **Imp1–3xHA binding proteins identified by mass spectrometry** *(Continued)*

PomBase accession no.	Gene	Imp1–3xHA	Control	Protein description
SPAC3A11.12c	**rpt5**	**1**	**0**	**19S proteasome regulatory subunit (predicted)**
SPAC222.12c	atp2	1	0	F1-ATPase β subunit
SPAC821.05	Unassigned	1	0	Translation initiation factor eIF3h
SPCC1827.03c	Unassigned	1	0	Acetyl-CoA ligase (predicted)
SPAC8C9.04	Unassigned	1	0	*S. pombe*–specific protein
SPCC18B5.01c	bfr1	1	0	Brefeldin A transmembrane transporter
SPBC428.04	apq12	1	0	Nuclear membrane organization protein (predicted)
SPCP25A2.03	Unassigned	1	0	THO complex subunit (predicted)
SPAC1D4.14	tho2	1	0	THO complex subunit (predicted)
SPBC651.01c	nog1	1	0	GTP binding protein (predicted)
SPAC30D11.03	ddx27	1	0	ATP-dependent RNA helicase (predicted)
SPAC15A10.09c	pun1	1	0	SUR7 family protein (predicted)
SPAC1F7.02c	has1	1	0	ATP-dependent RNA helicase (predicted)
SPAC12G12.02	efg1	1	0	rRNA processing protein (predicted)
SPBC216.01c	psy2	1	0	Protein phosphatase PP4 complex subunit
SPBC26H8.05c	pph3	1	0	Serine/threonine protein phosphatase, PP4 subunit
SPBC36.05c	clr6	1	0	Histone deacetylase (class I)
SPBC19F5.05c	ppp1	1	0	Pescadillo-family BRCT domain protein (predicted)
SPAC2F3.03c	rpa49	1	0	DNA-directed RNA polymerase I complex subunit
SPAC20G4.08	pdc1	1	0	mRNA decapping scaffolding protein
SPAC1834.03c	hhf1	1	0	Histone H4 h4.1
SPAC1805.08	dlc1	1	0	Dynein light chain
SPAC12G12.03	cip2	1	0	RNA-binding protein
SPBP8B7.20c	nop2	1	0	RNA methyltransferase (predicted)
SPAC24B11.06c	sty1	1	0	MAP kinase
SPBC3D6.02	but2	1	0	But2 family protein

In bold, proteins involved in nucleocytoplasmic transport and proteasome degradation. The number of non-redundant peptides found within each purification is shown.

Table S2. **Genotype and strain code of *S. pombe* strains used in this study**

Strain code	Genotype
RD313	h− ura4-d18 leu1-32 ade6-210
JJ1174	h− imp1Δ::ura4 leu1-32
JJ1801	h− cut11-GFP:ura4 SV40:GFP-atb2:leu1 sid2-Tom:nat^{r}
JJ1792	h− imp1Δ::ura4 cut11-GFP:ura4 SV40:GFP-atb2:leu1 sid2-Tom:nat^{r}
JJ1712	h− ura4-d18 ade6-210 SV40:GFP-atb2:leu1 sid2-Tom:nat^{r}
JJ1719	h− imp1Δ::ura4 SV40:GFP-atb2:leu1 sid2-Tom:nat^{r}
JJ1712	h− ura4-d18 ade6-210 SV40:GFP-atb2:leu1 sid2-Tom:nat^{r}
JJ1719	h− imp1Δ::ura4 SV40:GFP-atb2:leu1 sid2-Tom:nat^{r}
JJ1738	h− ura4-d18 leu1-32 imp1-GFP:kan^{r} sid2-Tom:nat^{r}
JJ1778	h− imp1-GFP:kan^{r} pREP81-tdTom-atb2
JJ1945	h− ura4-d18 leu1-32 ase1-GFP:kan^{r} imp1-Tom:nat^{r}
RD1233	h− ura4-d18 leu1-32 ase1-GFP:kan^{r} sid2-Tom:nat^{r}
JJ1779	h− ase1-GFP:kan^{r} imp1Δ::ura4 sid2-Tom:nat^{r}
JJ1889	h− imp1Δ::ura4 ase1::kan^{r} sid2-Tom:nat^{r} SV40:GFP-atb2:leu1
JJ1948	h+ leu1-32 cut15-GFP:kan^{r} imp1Δ::ura4 sid2-Tom:nat^{r}
JJ1900	h+ leu1-32 nup107-GFP:ura4 imp1-Tom:nat^{r}
JJ1912	h− imp1-Tom:nat^{r} nup61-GFP:ura4 ade6-210
JJ564	h− leu1-32 imp1-GFP:kan^{r}
JJ2205	h− imp1Δ::ura4 sid2-Tom:nat^{r} pREP41-GFP-imp1ΔIBB-ED (D192R E393R)
JJ2217	h− imp1-Tom pREP41-imp1ΔIBB-ED-GFP
JJ2218	h− imp1Δ::ura4 sid2-Tom:nat^{r} pREP41-GFP-imp1ΔIBB
JJ2241	h90 ade6-216 leu1-32 lys1-131 ura4-D18 kap104::kap104-GFP-HA:kan^{r}
JJ2243	h90 ade6-216 leu1-32 lys1-131 ura4-D18 sal3::sal3-GFP-HA:kan^{r}
JJ2156	h− imp1-GFP:ura4 pim1-d1 sid2-Tom:nat^{r}
JJ1738	h− ura4-d18 leu1-32 imp1-GFP:kan^{r} sid2-Tom:nat^{r}
JJ1712	h− ura4-d18 ade6-210 SV40:GFP-atb2:leu1 sid2-Tom:nat^{r}
JJ1992	h− pim1-d1 SV40:GFP-atb2:leu1 sid2-Tom:nat^{r}
JJ1712	h− ura4-d18 ade6-210 SV40:GFP-atb2:leu1 sid2-Tom:nat^{r}
JJ1980	h− ura4-d18 cdc48-353 SV40:GFP-atb2:leu1 sid2-Tom:nat^{r}
JJ1991	h− ura4-d18 leu1-32 cdc48-GFP:kan^{r}
JJ1983	h− leu1-32 imp1Δ::ura4 cdc48-GFP:kan^{r}
JJ1997	h− ura4-d18 leu1-32 pREP41-NLS* (LRAAAAP)-cdc48-GFP
RD1554	h− ura4-d18 leu1-32 ade6-210 ark1-GFP:kan^{r}
JJ1915	h− leu1-32 ark1-GFP:kan^{r} imp1Δ::ura4
JJ2070	h− ura4-d18 ade6-210 clp1-GFP:kan^{r}
PT432	h− ura4-d18 leu1-32 ade6-210 klp9-GFP:kan^{r}
JJ1806	h− leu1-32 klp9-GFP:kan^{r} imp1Δ::ura4
AR065	h− ura4-d18 klp5-GFP:kan^{r}pREP1-mRFP-atb2
RD3013	h+ int:pREP4x-SV40-NLS-GFP-lacZ:ura4 ade6- leu1-32 ura4-D18
RD3510	h+ rpn8-GFP:nat^{r} imp1-3xHA:kan^{r}
RD3513	h+ rpn8-GFP:nat^{r} imp1Δ::ura4 leu1-32
RD3250	h+ pim1-GFP:nat^{r} ade6-210 ura4-D18 leu1-32
JJ2361	h− pim1-d1 imp1-GFP:kan^{r}, nat^{r}:pADH-Cherry-atb2 leu1-32
JJ1892	h− ura4-d18 imp1Δ::ura4 klp5-GFP:kan^{r} pREP1-mRFP-atb2
AR085	h− ura4-d18 klp6-GFP:kan^{r}pREP1-mRFP-atb2
JJ1894	h− imp1Δ::ura4 klp6-GFP:kan^{r} pREP1-mRFP-atb2
JJ563	h− imp1-3xHA:kan^{r} leu1-32